Journal of Palaeogeography
2012, 1(1): 57-69
DOI: 10.3724/SP.J.1261.2012.00006

Palaeokarst

Origin and evolution of palaeokarst within the Lower Ordovician (Ibexian) Goodwin Formation (Pogonip Group)

Robert J. Kervin[1, 2], Adam D. Woods[1, *]

1. Department of Geological Sciences, California State University Fullerton, P.O. Box 6850, Fullerton, CA 92834-6850, USA
2. Wapiti Energy, 800 Gessner Rd., Suite 700, Houston, TX 77024, USA

Abstract Palaeokarst within the Lower to Middle Ordovician Goodwin Formation, Pogonip Group (upper Ibexian-lower Whiterockian) was examined in detail at Meiklejohn Peak, Nevada USA in order to determine its origin, evolution, and relationship to sea level change. Detailed outcrop and petrographic examination of dolostone breccias and host rock reveals that palaeokarst was formed and affected by two distinct cycles of sea level change. A relative transgression resulted in deposition of lagoonal, ooid shoal, and shallow subtidal facies as sea level rose. Exposure of the carbonate platform led to the formation of multiple phreatic caves below the water table, as well as the development of numerous vadose conduits from the downward percolation of meteoric waters. Vadose water flow through early cave-wall and cave-roof collapse breccias resulted in rounding of smaller breccias clasts via physical transport and corrosion, while subsidence of subsurface karst led to the formation of a palaeodoline at the exposure surface. A second relative transgression deposited lagoonal sediments over the older karst; subsequent re-exposure of the carbonate platform resulted in the development of small breccia pockets as well as grikes within the youngest lagoonal sediments, and may have led to further corrosion of the older, deeper subsurface karst. The distal location of the study area within the carbonate platform suggests karst formation was the result of a substantial drop in relative sea level; the presence of multiple generations of palaeokarst imply that at least two higher-frequency cycles of sea-level change overprint the larger regression.

Key words palaeokarst, Ordovician, carbonates, breccia, Great Basin

1 Introduction

Subaerial exposure and meteoric water flow through carbonate platforms during sea-level lowstands leads to carbonate dissolution and the development of unconformities expressed by palaeosols and the formation of surface and subsurface palaeokarst (Kendall and Schlager, 1981; Sarg, 1988). Many studies have documented and described palaeokarst in carbonate rocks of various ages from around the world (*e.g*., Roberts, 1966; Wright, 1982; Desrochers and James, 1988; Kerans, 1988; 1990; Kerans and Donaldson, 1988; Mussman *et al*., 1988; Pelechaty, *et al*., 1991; Mazzullo and Mazzullo, 1992; Jones and Hunter, 1994; Cooper and Keller, 2001), and the study of palaeokarst breccias has greatly increased our understanding of how this surface and subterranean process takes place, as well as the imprint it leaves behind on carbonate rocks. Palaeokarst has also been shown to have a practical application, as karst intervals have been utilized by numerous studies as sequence boundaries, since karst develops during periods of platform exposure (*e.g*., Canter *et al*., 1992; Knoll *et al*., 1995; Tinker *et al*., 1995;

* Corresponding author: Associate Professor.
Email: awoods@fullerton.edu.
Received: 2011-12-29 Accepted: 2012-02-20

Davies *et al*., 1997; D'Argenio *et al*., 1999; Clough and Goldhammer, 2000; Cooper and Keller, 2001; Palma *et al*., 2007). The Lower to Middle Ordovician (upper Ibexian to lower Whiterockian) Pogonip Group of the Great Basin, USA. contains multiple, laterally-extensive dolostone breccia bodies in eastern California and southern Nevada (Fig.1). These breccias have been interpreted as palaeokarst (Cooper and Keller, 1995; 2001), and were used, along with facies successions and stacking patterns, to develop a sequence stratigraphic framework for this region (Cooper and Keller, 2001). The current study expands the work of Cooper and Keller (1995; 2001) by scrutinizing a single palaeokarst package from the Ibexian Goodwin Formation (Pogonip Group) in detail at the outcrop, hand sample, and petrographic scale in order to better constrain its origin and evolution, and develop a detailed model for formation of the palaeokarst.

1.1 Geologic setting and background

A broad carbonate platform stretched across the southwestern United States from central Colorado to eastern California during much of the Ordovician (Ross, 1996). The Lower Ordovician (Ibexian) Goodwin Formation (Pogonip Group) of southern Nevada was deposited along the outer, western edge of this platform, and typically consists of dolomudstones, wackestones (dolostone and limestone), bindstones (dolostone and limestone), dolograinstones, and siltstones (Cooper and Keller, 1995; Ross, 1996). Decameter-scale depositional cycles within the Pogonip Group (including the Goodwin Formation) were linked to third- and fourth-order fluctuations in relative sea-level by Cooper and Keller (2001), who further suggested that breccias within the depositional cycles formed as the result of karstic processes. Cooper and

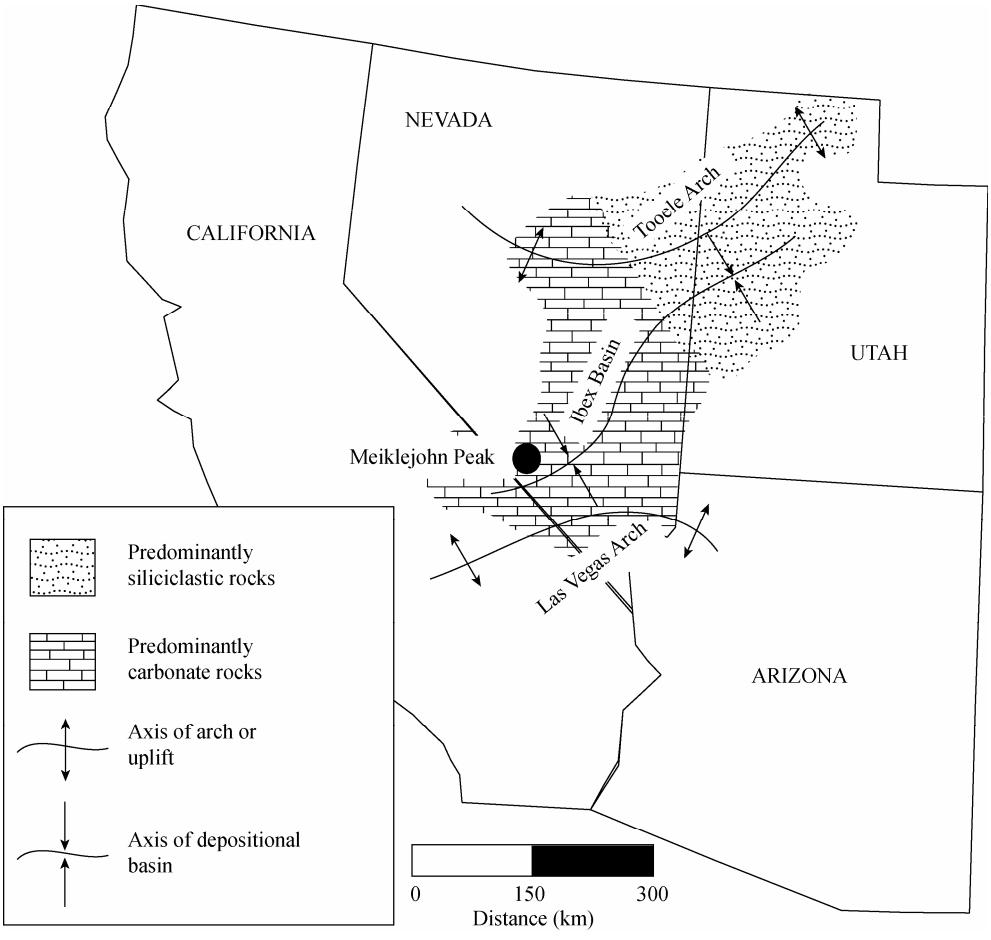

Fig. 1 Location of study area (Meiklejohn Peak, NV) and distribution of Lower Ordovician facies and palaeotectonic features in the southwestern United States (modified from Cooper and Keller, 2001)

Keller (1995; 2001) based this interpretation on several lines of evidence, including: 1) the breccias cross-cut primary depositional fabric and often have aberrant lithosome morphologies and irregular boundaries; 2) the breccias are typically chaotic, but locally display crackle fabrics (*i.e.*, fracturing has formed clasts, but the clasts are essentially in place) and mosaic fabrics (*i.e.*, fitted, angular clasts exhibiting minor rotation), which are thought to form as the result of cave collapse processes (Kerans, 1990, 1993; Loucks and Hanford, 1992); 3) small breccia bodies are monomictic, and are comprised of lithologies of the surrounding bedrock, while large breccia bodies that cross-cut multiple bedrock units are polymictic with clast populations whose proportions shift vertically through the breccia body, probably as the result of collapse of successive layers as the karst cavity grew vertically; 4) sandstone-filled grikes that were likely opened during exposure of the carbonate platform and filled with fluvial quartz sand and, 5) a variety of other sedimentologic features interpreted to have originated through karst processes, including karren, dolomite-filled vugs, and the local development of *terra rosa*. Once Cooper and Keller (2001) established a karstic origin for the dolostone breccias from the Pogonip Group, they suggested that the palaeokarst packages could be tied to sequence boundaries and utilized as a correlative framework for Ordovician strata in the region.

1.2 Study area

The Goodwin Formation (Pogonip Group) is exposed at Meiklejohn Peak, southwestern NV (Fig. 1), within Bare Mountain, a basin and range-type fault block composed primarily of Palaeozoic strata that have been thrust over younger Devonian rocks and are surrounded by Quaternary–Tertiary volcanics and sedimentary rocks (Cornwall and Kleinhampl, 1961; Ross, 1964, 1995). The Goodwin Formation at Meiklejohn Peak contains dolostone breccias that occur over an approximately 62 m-thick interval (Fig. 2), and are interpreted to be karstic in origin due to: 1) cross-cutting of primary depositional fabric by the breccia bodies; 2) the presence of crackle and mosaic fabrics within the typically chaotic breccias that occur in the study area (*e.g.*, Fig. 3A); 3) differences in clast lithologies between small, intrastratal breccia bodies, which tend to be monomictic, and large breccia bodies that cut across multiple strata and are polymictic (*e.g.*, Fig. 3B); and, 4) the presence vertical, dolomudstone-filled fissures at the top of the study interval that are interpreted to be grikes (see below).

2 Methods

The palaeokarst interval examined for this study comprises the uppermost 62 m of the Goodwin Formation exposed at Meiklejohn Peak and is bounded above by sequence boundary F (Goodwin Formation-Nine Mile Shale contact) of Cooper and Keller (2001). The study area was examined laterally over an approximately 10 m-wide swath, although gross lateral relationships and lithologic variability were ascertained over a width of 100 m or more. The palaeokarst interval was carefully investigated through detailed outcrop mapping and macroscopic examination of oriented drill cores (removed with a portable, gas-powered rock drill) and hand samples. Cores and hand samples were slabbed and particular attention was paid to clast shape, clast lithology, fabric, cement, porosity and solution features. Breccias were sampled preferentially; however, host rock also was sampled in order to determine the composition of the surrounding, undisturbed bedrock. Thirty-one oriented thin sections were made from the drill cores and were examined petrographically as well as under CL using a Luminoscope ELM-3R. Samples were viewed at 15–20 kV and under 100 millitorr of vacuum.

3 Results

Petrographic and macroscopic examination reveals five distinct depositional packages within the study interval, which are labeled Packages A through E (Fig. 2). Packages B-E have been replaced by dolomite, which obscures original textures, however, the diffusion technique of Delgado (1977) and the white card technique of Zenger (1979) allows the determination of precursor lithologies. Two main dolostone textures are present in the study interval: 1) finely crystalline (crystals range in size from 0.05–0.1 mm), equigranular, xenotopic dolomite that has replaced mudstones and peloidal mudstones (hereafter referred to as “dolomudstone” or “peloidal dolomudstone”); and, 2) slightly coarser crystalline (crystals range in size from 0.1–0.3 mm), equigranular, xenotopic dolomite that has replaced peloidal grainstones and oolitic grainstones (hereafter referred to as “peloidal” or “oolitic dolograinstone”). Breccias found within the study interval are clast-supported, and consist of dolomudstone and/or dolograinstone clasts surrounded by drusy, inequigranular, hypidiotopic dolomite cements with occasional saddle dolomite occurring as the last stage of

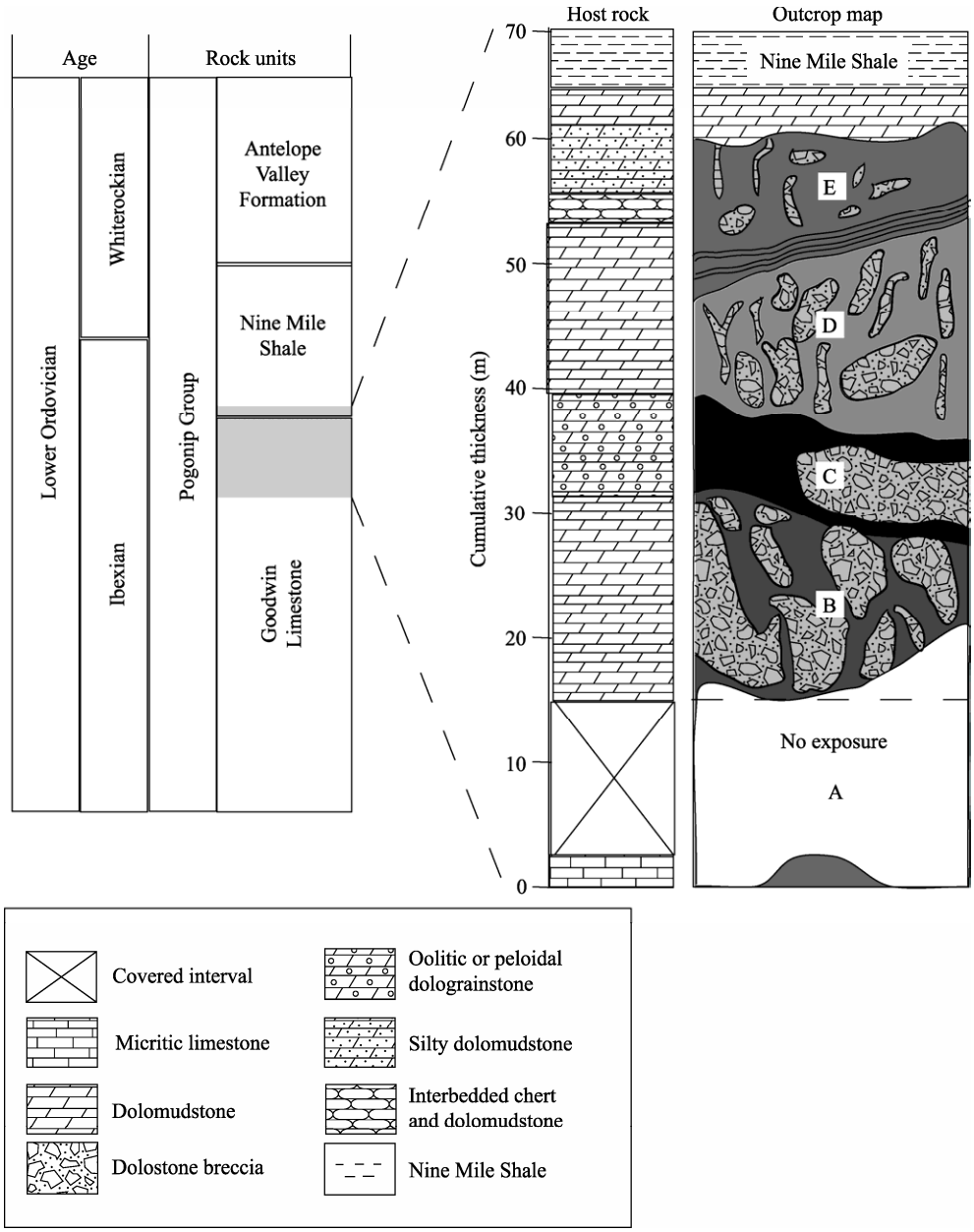

Fig. 2 Regional stratigraphy and age of the Pogonip Group in southwestern Nevada
Measured section through the karst interval showing host rock lithology, and outcrop map of study area showing the distribution of host rock and brecciated units; Width of outcrop map = 10 m.

cement growth. Siliciclastic matrix is relatively rare within the breccias, with the exception of Package E, where terrigenous material, in the form of clay and silt- to fine sand-sized quartz grains, becomes more common within the host rock, breccia clasts, and matrix.

1) *Package A*

Package A is poorly exposed due to vegetative overgrowth and talus cover. The unit is comprised of grey mudstone that exhibits wavy bedding. Beds are approximately 10 cm thick and are separated by thinly bedded (less than 1 cm), tan to brown argillaceous mudstone. There are no breccias in this portion of the study area; in addition, this is the only portion of the described sequence that has not been dolomitized.

2) *Package B*

The first exposure of Package B is located 13 m above the top of Package A (the intervening strata are covered by talus). The total package thickness is approximately 18.5 m, and consists of medium grey, interbedded laminated dolomudstone and medium grey, peloidal dolomudstone.

The lowest breccias in Package B appear just above the base of the exposure; however, because the contact

between Package A and Package B is covered, it is difficult to determine the true base of the breccias. The breccias in the lower 5 m of the unit occur as irregular, dm-scale bodies comprised of finely laminated dolomudstone and peloidal dolomudstone clasts, similar to the host rock (Fig. 3A). Breccia clasts range from 1.0 mm to approximately 50 mm in diameter, with most clasts less than 25 mm in diameter. Smaller clasts (1–15 mm) are subrounded to subangular, whereas clasts that are greater than 15 mm in diameter are angular to subangular.

Brecciation becomes more widespread above the lowermost 5 m of the unit; in some places, it is difficult to decipher between *in situ* host rock and large breccia clasts. Distinguishable breccia clasts range in size from 1.0 mm to several meters; smaller clasts (1–15 mm) are subrounded to subangular; larger clasts (>15 mm) are angular to subangular. Clasts within this interval are polymictic (Fig. 3B), and include: 1) thinly laminated, light to medium grey dolomudstone (10% of total); 2) massive, light to dark grey peloidal dolomudstone (80% of total); and 3) medium-dark grey oolitic dolograinstone (10% of total and likely derived from Package C).

A distinct change occurs with respect to the breccias in the upper 2 m of Package B where breccia clasts consist entirely of medium-dark grey, oolitic dolograinstone (derived from Package C). The breccia clasts are predominantly subangular-angular, ranging in size from 1.0 mm to approximately 6.0 cm. In addition, minor amounts of ooids occur within the dolomudstone host rock.

3) *Package C*

Package C is 7 m thick and consists of bedded, medium to dark grey, oolitic dolograinstone (Fig. 4A; ooids range in size from 0.25–0.75 mm in diameter). Package C varies laterally, and ranges from locally undisturbed strata to brecciated strata; breccias in the study area are contained within an elliptical-shaped body. Breccia clasts generally have the same lithology as the host bedrock and exhibit a very wide range of sizes from 1.0 mm to 5 m in diameter (Fig. 4B). One very large clast, 5 m in diameter, is comprised of light to medium grey dolomudstone

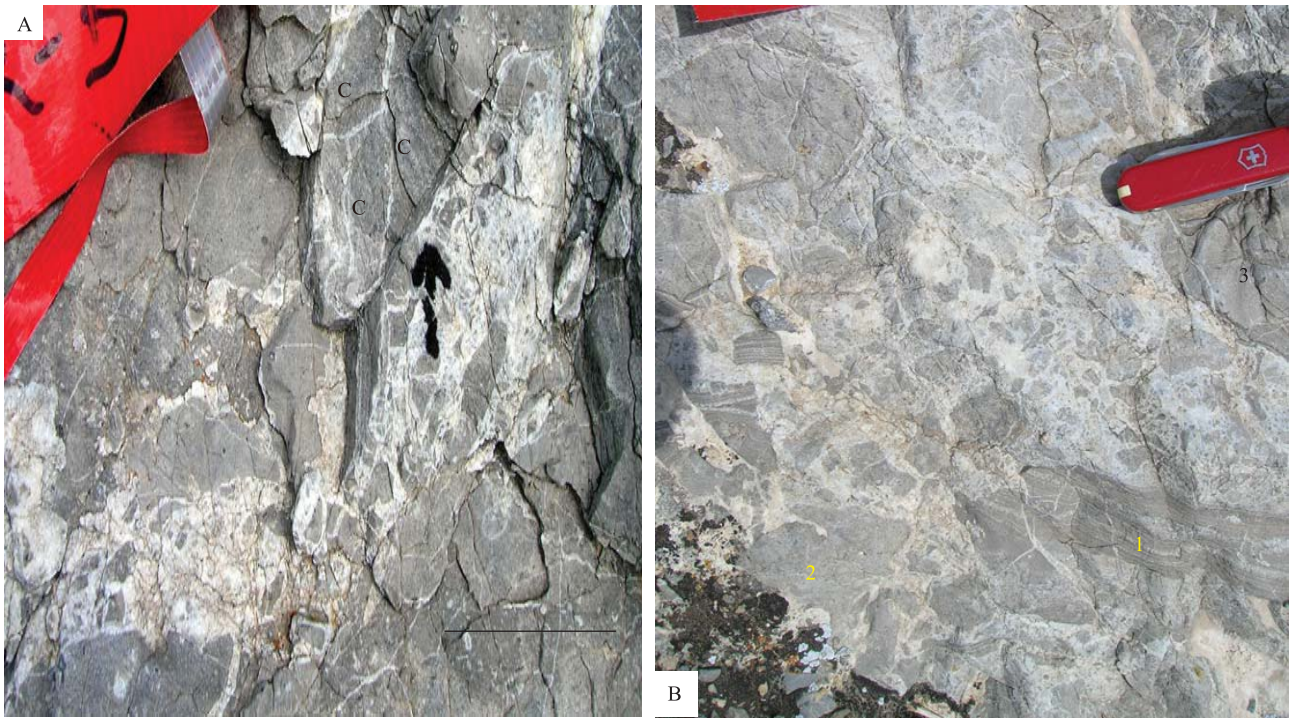

Fig. 3 Palaeokarst from Package B

A–Small, dm-scale breccia pocket near the base of Package B. Host rock and breccia clasts consist of medium grey, finely crystalline dolomudstone and peloidal dolomudstone. Breccia clasts range in size from 1.0 mm to approximately 50 mm in diameter, with most clasts less than 25 mm in diameter. Note crackle breccias (C) at the top of the breccia pocket, which imply a karstic origin for the breccias. Scale bar = 5 cm; B–Three different types of breccia clasts occur within the central portion of Package B (from approximately 5–13 m above the base), including: (1) finely laminated, light to medium grey dolomudstone; (2) massive, light to dark grey, fine to medium crystalline dolomudstone; and, (3) medium to dark grey dolomudstone. Polymictic breccia clast lithologies from multiple stratigraphic levels also imply a karstic origin for the breccias. Swiss Army knife is 6 cm in length.

breccia with a mosaic fabric and formed outside of the immediate vicinity based on the difference in lithology between the clast and the host rock. Large clasts (greater than approximately 5 cm) are subangular to angular; smaller clasts (less than 5 cm) are subangular to subrounded, matrix supported, and poorly sorted (Fig. 4C).

4) *Package D*

Package D is approximately 15 m thick and consists of interbedded peloidal dolograinstone and oolitic dolograinstone with rare beds of dolomudstone. Breccia clasts have the same lithology as the host rock; the proportion of clast lithologies is similar to their proportions in the host rock. Breccia clasts range in size from 1.0 mm to approximately 40 cm, and are subrounded to angular. Breccias in this package typically occur within vertically-oriented pipes (Fig. 5) that are often intertwined with each other; the pipes range in width from several cm to 1 m or more across, and may span several m vertically, but do not appear to cross the lower boundary with Package C.

5) *Package E*

Package E is approximately 8.5 m thick. The base of Package E consists of an approximately 1.5 m to 2 m-thick unit comprised of interbedded chert and dolomudstone (beds approximately 3 cm thick), that drape over the boundary with Package D, and exhibit growth strata (*i.e.*, the beds grow thicker in one direction) (Fig. 6). The chert and dolomudstone beds are cut by vertical faults in places and are overlain by angular chert and dolomudstone breccia clasts. The remainder of Package E consists of reddish dolomudstone that contains small pockets ($\leqslant$1 m across) of chaotic breccia (Fig. 7A) or mosaic breccia (Fig. 7B). Breccia clasts have the same composition as the surrounding host rock, are 1.0 mm to 5.0 cm in size, and

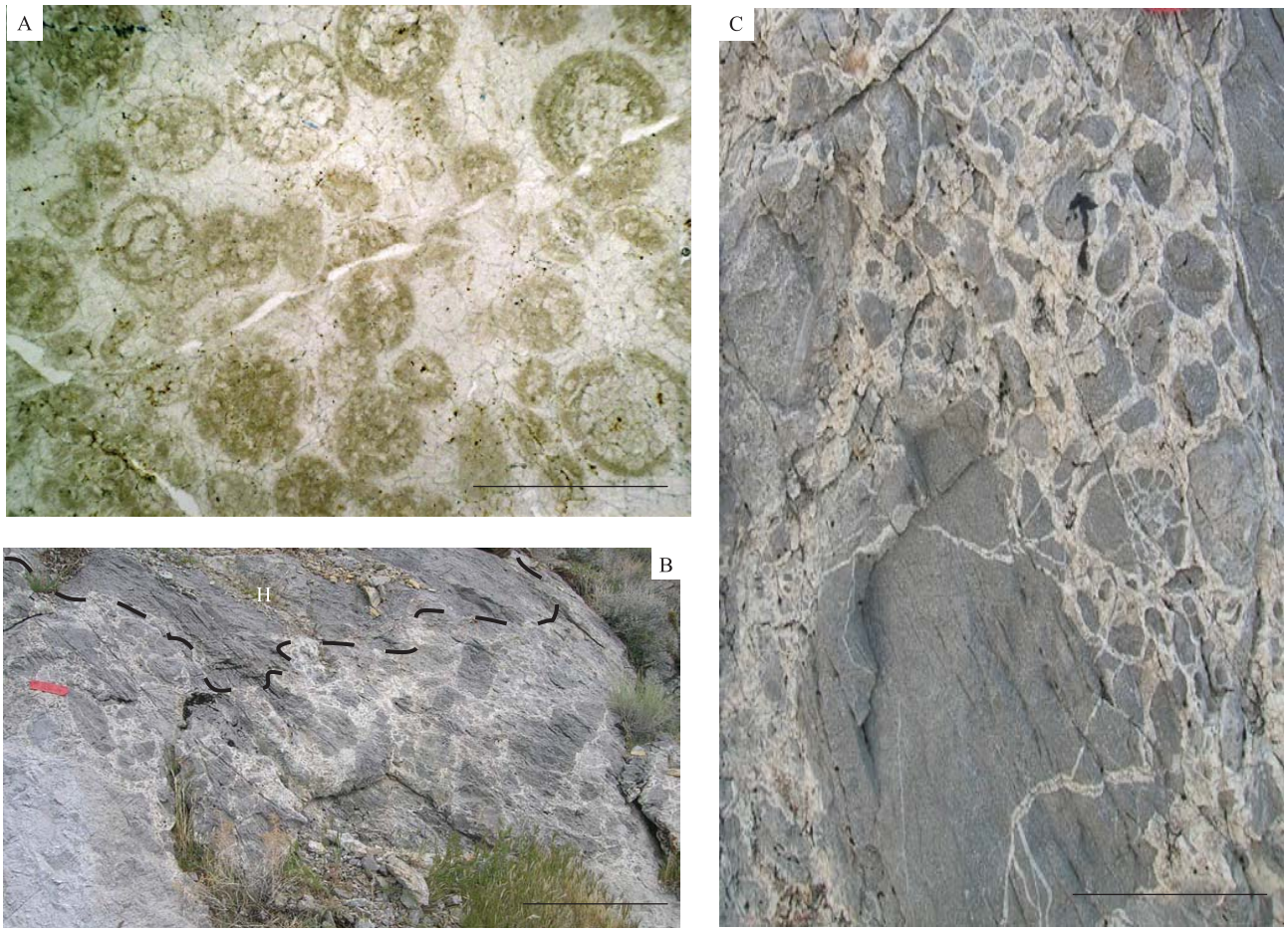

Fig. 4 Palaeokarst from Package C

A–Oolitic dolograinstone that comprises most of Package C. Ooids are 0.25–0.75 mm in diameter, and have been replaced by equigranular, xenotopic, 0.1–0.3 mm dolomite crystals. Scale bar = 1 mm. Diffuse light; B–A large, chaotically filled karst cavity; breccia clasts exhibit a wide range of sizes from 1.0 mm to 5.0 m. The dashed black line denotes the irregular upper boundary between the cavity and the host rock (H). Scale bar = 1 m; C–Smaller breccia clasts within Package C exhibit a greater degree of rounding than the larger breccia clasts and appear to be crudely sorted, probably as the result of vadose water flow through the subsurface. Scale bar = 10 cm.

Fig. 5 Characteristics of Package D
Breccias within Package D typically occur within vertically oriented pipes that likely formed as meteoric waters were pulled by gravity through exposed carbonate. Pen is 6 cm in length.

are angular to subangular. The upper boundary of Package E is demarcated by a breccia layer comprised of angular to subangular dolomudstone and chert clasts, 1.0 mm to 30 cm across, with a similar lithology to that of the overlying unit (Nine Mile Shale). In addition, dolomudstone-filled fissures cut downwards from the upper boundary of Package E; the fissures may be up to 20 cm wide, and cut up to 2 m downward into Package E. The dolomudstone that fills the fissures is not brecciated and is similar to the dolomudstone that comprises the overlying facies at the base of the Nine Mile Shale.

4 Interpretation

Outcrop and petrographic examination suggests that deposition of Packages A–E took place in nearshore carbonate settings ranging from lagoon to ooid shoal to shallow subtidal. The lime mudstones of Package A and

Fig. 6 Chert beds at the base of Package E display growth strata that are interpreted to have been deposited on the surface of a subsiding palaeodoline. The dashed lines outline some of the chert beds. (GS = growth strata)

the dolomudstones of Packages B and E are thought to have been deposited in a quiet lagoonal setting; scattered ooids near the top of Package B were washed into the lagoon by storms. The oolitic dolograinstones of Package C were likely deposited as an ooid shoal located seaward of the lagoon that resulted in the development of quiet conditions where lime mud was deposited. The interbedded oolitic dolograinstones and peloidal dolograinstones of Package D also imply deposition in a high-energy environment, perhaps in a shallow subtidal setting seaward of the ooid shoal. Overall, the sequence of facies represented by Packages A–D implies a relative rise in sea-level.

The appearance of breccia clasts near the base of Package B suggests that lowest extent of palaeokarst is likely found there. Breccia clasts within Package B are primarily comprised of lithologies similar to that of the host rock (90% of all clasts), but the breccias also contain oolitic dolograinstone clasts that appear to have been derived from Package C (10% of all clasts). The presence of clasts from Package C within Package B is indicative of the former presence of a deep, perhaps multi-tiered palaeocave system that cut across multiple strata, and formed as the result of a fluctuating water table. Breccias within the upper 2 m of Package B that are comprised entirely of angular clasts from Package C represent a breakdown breccia, or a breccia that formed during burial when compaction led to the collapse of the cave roof into an open cavity at the top of Package B (*e.g.*, Kerans, 1988, 1993; Loucks and Handford, 1992; Loucks, 1999).

Large, dm- to m-scale clasts within palaeokarst breccias, similar to those found in Packages B and C, have

been interpreted by other authors to be a product of cave-roof and cave-wall collapse (*e.g.*, White and White, 1969; Loucks and Handford, 1992; Loucks, 1999). Upon impact, many large clasts shatter into smaller pieces to form breakdown clasts (*e.g.*, Loucks and Handford, 1992; Loucks, 1999;), and this is the probable origin for the smaller clasts found in Packages B and C. Evidence for this origin includes crackle brecciation along the outer edges of the larger clasts (Loucks and Handford, 1992; Loucks, 1999), and lithologic similarities between the larger and smaller clasts. The smaller clasts in Packages B and C (as well as in Package D) typically exhibit some degree of rounding, and, in some areas, the smaller clasts are crudely sorted, implying transport of the smaller clasts by vadose water flow (Bögli, 1980). Rounding may also be related to corrosion of the clasts by CO_2-charged vadose waters (de Wet *et al*., 1997; Kwon *et al*., 2002); sorting of the breccia clasts implies that at least some of the rounding was the result of transport. Vadose flow through caves is common but typically sporadic (*e.g.*, Ford, 1988; Palmer, 1991; White, 2006); if flow from the surface were constant, the complete dissolution of the carbonate breccias would have occurred. When vadose waters reached an area of the cave that was filled with larger clasts as the result of cave roof or cave wall collapse (such as in the study area), the increased roughness of the subterranean channel slowed the flow of vadose waters, and the smaller, rounded clasts were deposited in the interstices between the larger clasts. An increase in the size of clasts exhibiting some degree of rounding from Package B (< 1.5 cm) to Package C (< 5 cm) suggests that water velocities in Package B were much lower than those in Package C.

Package D has a sharp lower boundary with Package C, and the type of palaeokarst is significantly different from below. The karst cavities in Package D are not as large as those observed in Packages B and C, and are much more conduit-like in appearance. While this change in karst morphology may be due to lithologic differences, a more likely scenario is that the rocks that comprise Package D were located within the vadose zone during platform exposure, and conduit morphologies formed as the result of gravity pulling CO_2-charged meteoric waters downwards through exposed carbonate (*e.g.*, Bögli, 1980; James and Choquette, 1984; Choquette and James, 1988; Ford, 1988; Palmer, 1991; Loucks, 1999; Ford and Williams, 2007). These cavities do not appear to have been open to the surface since they are not plugged with sediment from overlying facies. Rounding of breccias clasts within Package D likely occurred as vadose waters flowed through the conduits during a second period of exposure of the carbonate platform following deposition of Package E.

Package D is overlain by interbedded chert and dolomudstone that occur at the base of Package E; these overlying beds exhibit growth strata that apparently formed as the sediments were deposited on a subsiding substrate, probably a doline (Fig. 6). Continued collapse of deeper cavities in Packages B and C following lithification is suggested by parallel vertical faults that cut through bedding in the lower 2 m of Package E, and may have aided in the formation of cavities within the upper portion of Package E (see below).

Palaeokarst cavities occur throughout the remainder of Package E, although they are small (⩽1 m), localized, and much less prominent than the karst cavities in the underlying packages. Mosaic breccias within some of the cavities suggest that tensional stresses from underlying cave collapse and concomitant loss of structural support played a role in opening the cavities (Fig. 7B). Dissolutional processes from meteoric waters further modified the cavities as vadose waters percolated downwards through Package E. In addition, fissures, interpreted as grikes, cut up to 2 m downwards from the upper boundary of Package E. Grikes form as meteoric waters percolate downwards through joint systems, allowing infiltration of overlying sediments (Bögli, 1980; James and Choquette, 1984; Desrochers and James, 1988); in this case, the fissures in Package E are filled with dolomudstone similar to that which comprises the lowermost Nine Mile Shale in the area, suggesting that the fissures were open to the surface. The top of Package E is covered with a breakdown breccia comprised of clasts of the overlying lithology (dolomudstones of the lowermost Nine Mile Shale) that collapsed during burial and compaction into the irregular underlying topography created by the deeper collapse of karst cavities within Packages B and C (and, perhaps D).

5 Palaeokarst model

Examination of host rock and palaeokarst in outcrop, hand samples, and in thin section suggests carbonate deposition and development of the palaeokarst in the study area occurred as the result of two cycles of sea level change. Following deposition and karstification, post-depositional processes continued to affect and mod-

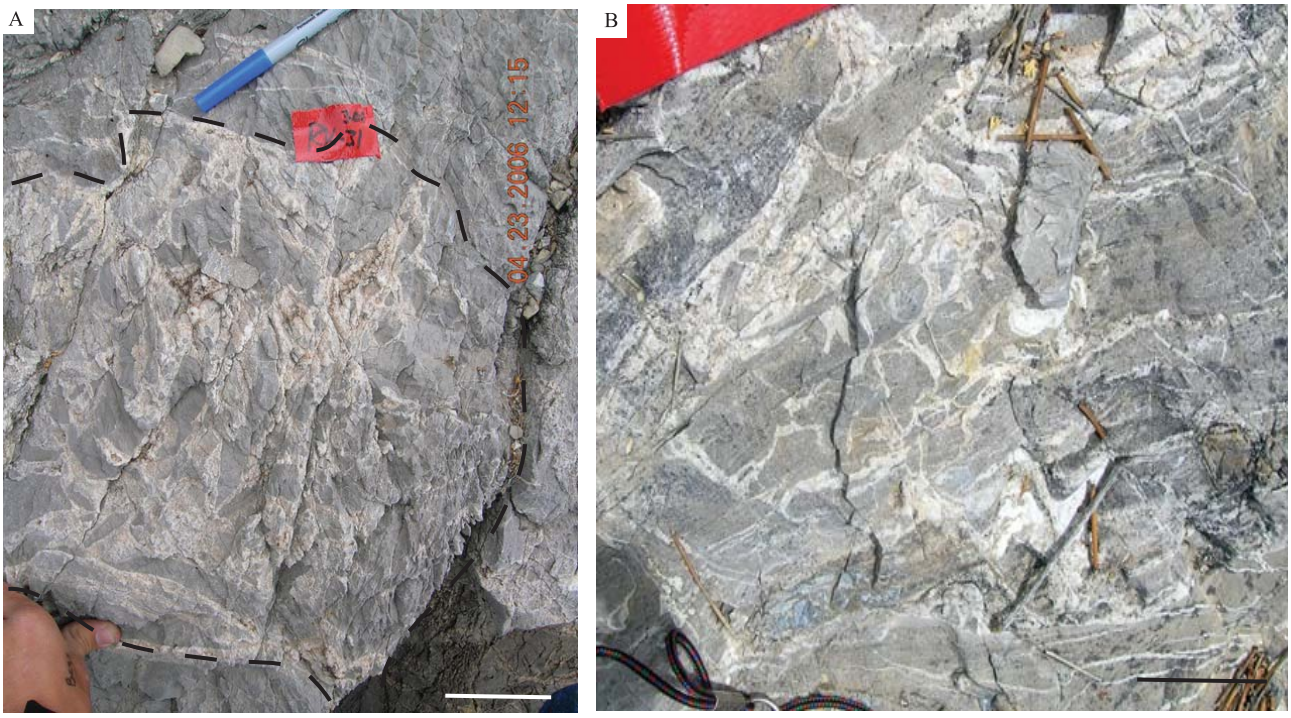

Fig. 7 Palaeokarst cavities within Package E may be filled with chaotic breccias as in A (the dashed black line outlines the edge of the cavity) or by mosaic breccias as in B. Cavity formation was likely the result of the combination of a loss of structural support from below which opened the cavities via tensional stress and corrosion from vadose water flow through the cavities. Scale bar in both photographs = 5 cm.

ify the palaeokarst package.

5.1 Sequence 1

The vertical progression of facies from Package A through Package D is interpreted to represent a relative transgression and lateral migration of sedimentary environments from quiet lagoonal facies (the lime mudstones of Package A and the dolomudstones of Package B) to ooid shoal (oolitic dolograinstones of Package C) to a shallow subtidal setting along the seaward face of the ooid shoal (interbedded oolitic dolograinstones, peloidal dolograinstones, and rare dolomudstones of Package D); Package D is interpreted to be the maximum flooding interval (Fig. 8, step 1). Following deposition of Package D, sea-level dropped, and the platform was exposed. Meteoric waters percolated downward through the exposed carbonate platform to the phreatic zone. The presence of breccia conduits, as opposed to large, irregular breccia pockets, in Package D suggests that the water table was located below Package D (Fig. 8, step 2); the water table likely fluctuated between a level in Package B and Package C, and led to dissolution of limestone and formation of caves at different levels. An elliptical-shaped palaeokarst body within Package C implies the presence of a phreatic tube that was separate from the more cavernous karst below in Package B; however, the occurrence of oolitic dolograinstone clasts that were likely derived from Package C within Package B suggests that the two packages were part of a larger, connected, multi-tiered cave system. The large karst cavities within Packages B, C, and perhaps D appear to have been partially filled with breccias from cave-roof and cave-wall collapse during one or possibly both of the episodes of platform exposure, and the flow of vadose waters through the cave system led to rounding of small breccia clasts. Collapse of the cave roof also led to the establishment of the palaeodoline at the top of Package D from a lack of underlying structural support. Karstification came to an end when sea-level rose and Package E was deposited.

5.2 Sequence 2

A relative rise in sea-level led to the deposition of the lagoonal sediments over the irregular karst surface at the top of Package D (Fig. 8, step 3). Karst cavities within Packages B–D continued to collapse and subside, filling the cavities with breccias, and leading to the formation of

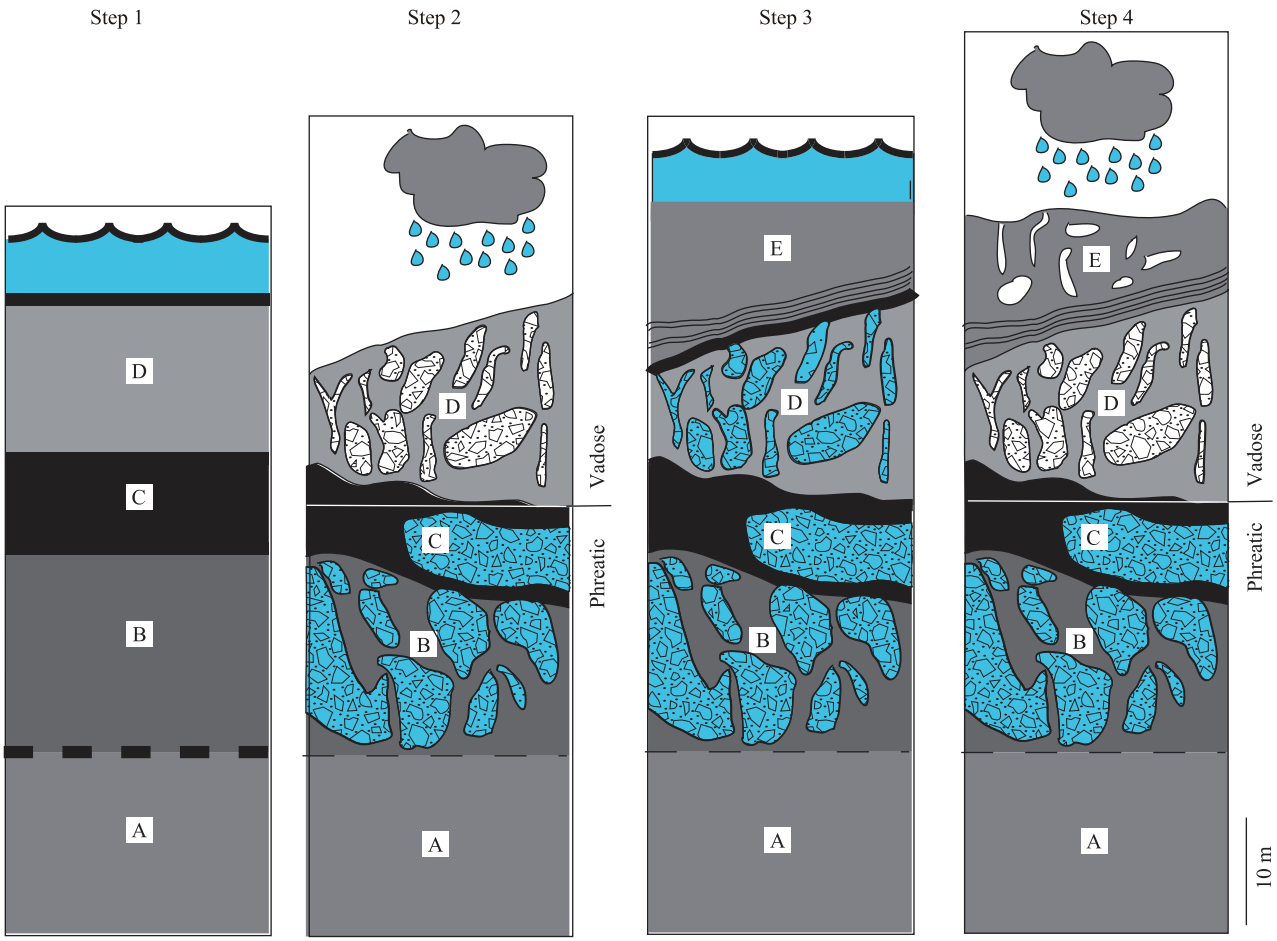

Fig. 8 Model of karst formation in the study area

Step 1: Deposition of Packages A through D during the initial relative transgression. Step 2: A relative regression led to exposure of the carbonate platform and the formation of linear cavities in Package D as CO_2-charged waters percolated downwards to the phreatic zone and the concomitant formation of the large karst cavities in Packages B and C via interaction with phreatic waters. The doline probably began to form during this time as the result of a loss of structural support from cave collapse at deeper levels. Step 3: Flooding of the carbonate shelf during a second transgression resulted in the deposition of interbedded cherts and mudstones over the doline. Continued collapse of karst cavities at deeper levels led to the formation of growth strata in the cherts and dolomudstones as they were deposited on a subsiding surface. Mudstone was subsequently deposited on top of the sequence, forming the host rock of Package E. Step 4: The platform was exposed a second time, resulting in the formation of small karst cavities and grikes in Package E. Re-exposure of the carbonate platform also likely led to further cave-roof and cave-wall collapse within Packages B, C and D, and this loss of underlying structural support also played a role in opening the small karst cavities in Package E. The entire sequence was subsequently buried by deposition of the Nine Mile Shale, and breakdown breccias and cement infilled the remaining pore spaces.

growth strata over the palaeodoline in the lower 2 m of Package E. The growth strata imply slow subsidence of the substrate as opposed to a catastrophic collapse; the presence marine phreatic waters likely provided some support for the bedrock in the subterranean cavity system during the second transgression (White and White, 1969).

A regression followed the deposition of Package E and led to the further development of karst (Fig. 8, step 4). Continued collapse of underlying caverns reduced support for overlying sediments, and resulted in the physical opening of the small overlying cavities in Package E, which were filled with mosaic or chaotic breccias and widened by vadose corrosion. Loss of underlying structural support also led to normal faulting of the interbedded chert and dolomudstones at the base of Package E. Platform exposure led to widening of joints by percolating meteoric fluids, which were later filled with dolomudstone that infiltrated from above to form grikes. A third relative transgression led to the burial of the underlying karst system via deposition of overlying dolomud-

stones and shales of the Nine Mile Shale.

5.3 Burial modification of karst

As mentioned above, most of the breccias in the study area appear to have formed prior to burial of the sequence as the result of cave roof and cave wall collapse, however, some brecciation did occur at depth. Breakdown breccias are found along the upper boundaries of Package B, Package D, and Package E, as well as at the top of the interbedded cherts and dolomudstones at the base of Package E, and formed as burial compaction resulted in collapse of bedrock into open cavities (*e.g.*, Kerans, 1988, 1993; Loucks and Handford, 1992; Loucks, 1999). This origin is supported by the angular nature of the cave-roof collapse breccias, which suggests that they were not exposed to vadose water flow, but were instead formed at depth. Drusy cementation of the breccia clasts, coupled with a typically dull luminescence under CL and the occurrence of baroque dolomite as the final cement stage suggests that cement growth occurred at burial depths (*e.g.*, Grover and Read, 1983; Harris, *et al.*, 1985; Scholle and Halley, 1985; Choquette and James, 1987; Flügel, 2004). Some cement exhibits a late, zoned CL pattern between bright orange and dull luminescent orange suggesting shifting redox or pH conditions in pore water chemistry at depth (*e.g.*, Grover and Read, 1983; Moore, 1985, 1989; Scholle and Halley, 1985; Choquette and James, 1987;). Occasional early cementation of breccias apparently occurred, as suggested by a single-5-m diameter boulder in Package C that consists of dolomudstone breccia with a mosaic fabric that presumably formed and lithified elsewhere, likely by cementation of a cave-roof collapse breccia (*e.g.*, Loucks and Handford, 1992; Loucks, 1999).

6 Conclusions

This study documents what is perhaps the first example of rounding of carbonate clasts by vadose water flow. Palaeokarst breccias are typically angular, and undergo little, if any, transport beyond falling from the cave roof to the cave floor. The subrounded clasts of Package B, C and D suggests that under the right conditions (*i.e.*, early cave roof and cave wall collapse and sporadic vadose water flow), small carbonate clasts may be transported by vadose water flow through cave systems and undergo a moderate degree of rounding.

Surface and subsurface karst development was relatively common within the vast carbonate depositional systems that covered a large portion of Laurentia during the Ordovician (e.g., Desrochers and James, 1988; Kerans, 1988; Mussman *et al.*, 1988; Dix *et al.*, 1998; Cooper and Keller, 2001; Smosna *et al.*, 2005). Within the southern Great Basin, regional tectonic activity associated with the Las Vegas Arch, coupled with eustatic variations in sea level, are hypothesized to have led to repeated exposure of the platform to meteoric waters (Cooper and Keller, 2001). The study area (Meiklejohn Peak) was located along the distal edge of the carbonate platform during the Ordovician (Ross *et al.*, 1989; Ross, 1996); therefore, exposure and karstification of the platform required a substantial drop in relative sea-level, on the order of tens of meters to 100 m or more. The presence of two distinct episodes of platform exposure suggests that the regression that led to the exposure of the distal portion of the carbonate platform involved two smaller-scale fluctuations in relative sea-level, and may be the result of either higher-frequency eustatic sea-level changes nested within a longer cycle of sea-level change, or may represent tectonic activity that overprinted the longer eustatic signal.

Acknowledgements

AAPG Grants-In-Aid funding provided financial support for this research (Kervin). We thank Frank Corsetti (University of Southern California) for providing access to his cathodoluminescence microscope. Phil Armstrong and Matt Kirby provided valuable guidance to this project while still in the M.S. thesis stage. John Cooper read early versions of this manuscript and provided invaluable advice and expertise that greatly strengthened this paper.

References

Bögli, A., 1980. Karst hydrology and physical speleology. Springer-Verlag, Berlin, 284.

Canter, K. L., Wheeler, D. M., Geesaman, R. C., 1992. Sequence stratigraphy and depositional facies of the Siluro-Devonian interval of the northern Permian Basin. In: Candelaria, M. P. and Reed, C. L. (eds). Paleokarst, Karst-Related Diagenesis, and Reservoir Development: Examples from Ordovician-Devonian Age Strata of West Texas and the Mid-Continent. Permian Basin Section SEPM Publication, 92–33, 93–109.

Choquette, P. W., James, N. P., 1987. Diagenesis #12. Diagenesis in limestones – 3. The deep burial environment. Geoscience Canada, 14: 3–35.

Choquette, P. W., James, N. P., 1988. Introduction. In: James, N. P.

and Choquette P. W. (eds). Paleokarst, 1–21. Springer-Verlag, New York.

Clough, J. G. , Goldhammer, R. K., 2000. Evolution of the Neoproterozoic Katakturuk Dolomite ramp complex, northeastern Brooks Range, Alaska. In: Grotzinger J. P. and James N. P. (eds). Carbonate Sedimentation and Diagenesis in the Evolving Precambrian World, SEPM Spec. Publ., 67: 209–241.

Cooper, J. D., Keller, M., 1995. Ordovician craton margin-miogeoclinal transition, southern Great Basin. In: Cooper J. D. (ed.). Ordovician of the Great Basin: Field Trip Volume and Guidebook for the 7th International Symposium on the Ordovician System, Pacific Section SEPM Book, 78: 107–132.

Cooper, J. D., Keller, M., 2001. Palaeokarst in the Ordovician of the southern Great Basin, USA: Implications for sea-level history. Sedimentology, 48: 855–873.

Cornwall, H. R., Kleinhampl, F. J., 1961. Geology of the Bare Mountain Quadrangle, Nevada. United States Geological Survey, Washington, D. C., Map GQ–157.

D'Argenio, B., Ferreri, V., Raspini, A., Amodio, S., Buonocunto, F. P., 1999. Cyclostratigraphy of a carbonate platform as a tool for high-precision correlation. Tectonophysics, 315: 357–384.

Davies, G. R., Moslow, T. F., Sherwin, M. D., 1997. The Lower Triassic Montney Formation, west-central Alberta. Bulletin of Canadian Petroleum Geology, 45: 474–505.

Delgado, F., 1977. Primary textures in dolostones and recrystallized limestones: A technique for their microscopic study. Journal of Sedimentary Petrology, 47: 1339–1341.

Desrochers, A., James, N. P., 1988. Early Paleozoic surface and subsurface paleokarst: Middle Ordovician Carbonates, Mingin Islands, Quebec. In: James, N. P. and Choquette, P. W. (eds). Paleokarst, Springer-Verlag, New York, 183–210.

de Wet, C. B., Moshier, S. O., Hower, J. C., de Wet, A. P., Brennan, S. T., Helfrich, C. T., Raymond, A. L., 1997. Disrupted coal and carbonate facies within two Pennsylvanian cyclothems, southern Illinois basin, United States. Geological Society of America Bulletin, 109: 1231–1248.

Dix, G. R., Robinson, G. W., McGregor, D. C., 1998. Paleokarst in the Lower Ordovician Beekmantown Group, Ottawa Embayment; structural control inboard of the Appalachian Orogen. Geological Society of America Bulletin, 110: 1046–1059.

Flügel, E., 2004. Microfacies of Carbonate Rock: Analysis, Interpretation and Application. Springer-Verlag, Berlin, 976.

Ford, D., 1988. Characteristics of dissolutional cave systems in carbonate rocks. In: James, N. P. and Choquette, P. W. (eds). Paleokarst, Springer-Verlag, New York. 25–57.

Ford, D., Williams, P., 2007. Karst Hydrology and Geomorphology. Wiley, Chichester, 562.

Grover, G., Read, J. F., 1983. Paleoaquifer and deep burial related cements defined by regional cathodoluminescent patterns, Middle Ordovician carbonates, Virginia. AAPG Bulletin, 67: 1275–1303.

Harris, P. M., Kendall, C. G. St. C., Lerche, I., 1985. Carbonate cementation - A brief review. In: Schneidermann, N. and Harris, P. M. (eds). Carbonate Cements. SEPM Spec. Publ., 26: 79–95.

James, N. P., Choquette, P. W., 1984. Diagenesis 9. Limestones-The meteoric diagenetic environment. Geoscience Canada, 11: 161–194.

Jones, B., Hunter, I. G., 1994. Messinian (late Miocene) karst on Grand Cayman, British West Indies: An example of an erosional sequence boundary. Journal of Sedimentary Research, 64: 531–541.

Kendall, C. G. S. C., Schlager, W., 1981. Carbonates and relative changes in sea level. Marine Geology, 44: 181–212.

Kerans, C., 1988. Karst-controlled reservoir heterogeneity in Ellenberger Group carbonates of west Texas. AAPG Bulletin, 72: 1160–1183.

Kerans, C., 1990. Depositional systems and karst geology of the Ellenberger Group, (Lower Ordovician), subsurface west Texas. University of Texas, Bureau of Economic Geology, Austin, TX, Report of Investigations, 193: 63.

Kerans, C., 1993. Description and interpretation of karst-related breccia fabrics, Ellenburger Group, west Texas. In: Wilson, J. L. and Yurewicz (eds). Paleokarst Related Hydrocarbon Reservoirs, SEPM Core Workshop, 18: 181–200.

Kerans, C., Donaldson, J. A., 1988. Proterozoic paleokarst profile, Dismal Lakes Group, N. W. T., Canada. In: James, N. P. and Choguette (eds). Paleokarst, Springer-Verlag, New York. 167-182.

Knoll, A. H., Grotzinger, J. P., Kaufman, A. J., Kolosov, P., 1995. Integrated approaches to terminal Proterozoic stratigraphy: An example from the Olenek Uplift, northeastern Siberia. Precambrian Research, 73: 251–270.

Kwon, Y. K., Chough, S. K., Choi, D. K., Lee, D. J., 2002. Origin of limestone conglomerates in the Choson Supergroup (Cambro-Ordovician), mid-east Korea. Sedimentary Geology, 146: 265–283.

Loucks, R. G., 1999. Paleocave carbonate reservoirs: Origins, burial-depth modifications, spatial complexity, and reservoir modifications, spatial complexity, and reservoir implications. AAPG Bulletin, 83: 1795–1833.

Loucks, R. G., Handford, C. R., 1992. Origin and recognition of fractures, breccias, and sediment fills in paleocave-reservoir networks, in paleocave-reservoir networks. In: Candelaria, M. P. and Reed, C. L. (eds). Paleokarst, Karst Related Diagenesis and Reservoir, Development: Examples from Ordovician-Devonian age Strata of West Texas and the Mid-Continent, Permian Basin Section SEPM Publ., 92–33, 31–44.

Mazzullo, S. J., Mazzullo, L. J., 1992. Paleokarst and karst- associated hydrocarbon reserviors in the Fusselman Formation, west Texas, Permian Basin. In: Candelaria M. P. and Reed C. L. (eds). Paleokarst, Karst-Related Diagenesis, and Reservoir Develop-

ment: Examples from Ordovician-Devonian Age Strata of West Texas and the Mid-Continent, Permian Basin Section SEPM Publ., 92–33, 110–120.

Moore, C. H., 1985. Upper Jurassic subsurface cements: A case history. In: Schneidermann N. and Harris, P. M. (eds). Carbonate Cements, SEPM Spec. Publ., 36: 291–308.

Moore, C. H., 1989. Carbonate Diagenesis and Porosity. Developments in Sedimentology, 46: Elsevier, Amsterdam, 338.

Mussman, W. J., Montanez, I. P., Read, J. F., 1988. Ordovician Knox paleokarst unconformity, Appalachians In: James N. P. and Choquette P. W. (eds). Paleokarst, Springer- Verlag, New York. 211-228.

Palma, R. M., Lopez-Gomez, J., Piethe, R. D., 2007. Oxfordian ramp system (La Manga Formation) in the Bardas Blancas area (Mendoza Province) Neuquén Basin, Argentina: Facies and depositional sequences. Sedimentary Geology, 195: 113–134.

Palmer, A. N., 1991. Origin and morphology of limestones caves. Geological Society of America Bulletin, 103: 1–21.

Pelechaty, S. M., James, N. P., Kerans, C., Grotzinger, J. P., 1991. A middle Proterozoic palaeokarst unconformity and associated sedimentary rocks, Elu Basin, northwest Canada. Sedimentology, 38: 775–797.

Roberts, A. E., 1966. Stratigraphy of Madison Group near Livingston, Montana, and discussion of karst and solution-breccia features. USGS Professional Paper, 526-B: 23.

Ross, R. J., 1964. Middle and Lower Ordovician Formations in Southernmost Nevada and Adjacent California. USGS Bulletin, 1180-C: 101.

Ross, R. J., 1995. Mid-symposium field trip: Las Vegas to Meiklejohn Peak near Beatty, Nevada. In: Cooper, J. D. (ed). Ordovician of the Great Basin: Field Trip Volume and Guidebook for the 7th International Symposium on the Ordovician System, Pacific Section SEPM Book, 78: 51–62.

Ross, R. J., 1996. Quintessence of the Ordovician: From Rocky Mountain Beaches to the Depths of Nevada. In: Longman, M. W. and Sonnenfeld (eds). Paleozoic Systems of the Rocky Mountain Region, Rocky Mountain Section SEPM, 47–62.

Ross, R. J., James, N., Hintze, L. F., Poole, F. G., 1989. Architecture and evolution of a Whiterockian (Early Middle Ordovician) carbonate platform, Basin Ranges of western USA. In: Crevello, P. D. *et al*., (eds). Controls on Carbonate Platform and Basin Development, SEPM Spec. Publ., 44: 167–185.

Sarg, J. F., 1988. Carbonate sequence stratigraphy. In: Wilgus, C. K. *et al*., (eds). Sea-level Changes: An Integrated Approach, SEPM Spec. Publ., 42: 155–181.

Scholle, P. A., Halley, R. B., 1985. Burial diagenesis: Out of sight, out of mind! In: Scheidermann, N. and Harris, P. M. (eds). Carbonate Cements, SEPM Spec. Publ., 36: 309–334.

Smosna, R., Bruner, K. R., Riley, R. A., 2005. Paleokarst and reservoir porosity in the Ordovician Beekmantown Dolomite of the central Appalachian Basin. Carbonates and Evaporites, 20: 50–63.

Tinker, S. W., Ehrets, J. R., Brondos, M. D., 1995. Multiple karst events related to stratigraphic cyclicity; San Andres Formation, Yates Field, West Texas. In: Budd, D. A. *et al*., (eds). Unconformities and Porosity in Carbonate Strata, AAPG Memoir, 63: 213–237.

White, E. L., White, W. B., 1969. Processes of cave breakdown. Bulletin of the National Speleological Society, 31: 83–96.

White, W. B., 2006. Fifty years of karst hydrology and hydrogeology: 1953-2003. In: Harmon, R. S. and Wicds, C. (eds). Perspectives on Karst Geomorphology, Hydrology, and Geochemistry - A Tribute Volume to Derek C. Ford and William B. White, Geological Society of America Special Paper, 404: 139–152.

Wright, V. P., 1982. The recognition and interpretation of paleokarsts: two examples from the Lower Carboniferous of South Wales. Journal of Sedimentary Petrology, 52: 83–94.

Zenger, D. H., 1979. Primary textures in dolostones and recrystallized limestones: A technique for their microscopic study. Journal of Sedimentary Petrology: 49, 677–678.

(**Edited by Wang Yuan, Zheng Xiujuan**)